Improving the Accuracy of Computational Fluid Dynamics Simulations of Nuclear Waste Mixing using Direct Numerical Simulations - 16260

Ahmadreza Abbasi Baharanchi, Maximiliano Edrei, Seckin Gokaltun, Dwayne McDaniel
Applied Research Center, Florida International University
10555 West Flagler Street, Suite 2100, Miami, FL 33174

ABSTRACT

Experimental evaluations of pulse-jet mixer (PJM) performance in handling high-level waste (HLW) is a big challenge due to the large number of variables and high cost associated with building and testing the mixing process in the tanks. Computational fluid dynamics (CFD) predictions using computer simulations of the multiphase flow physics by solving the governing equations for the gas-solid multiphase flow under turbulent flow conditions can be used to aid in the design estimations and performance scaling calculations. A reliable CFD simulation of the mixing process of the nuclear waste slurry in the storage tanks using pulse-jet mixers requires correct representation of the viscoplastic material properties of the nuclear sludge.

In this work, Reynolds-averaged Navier-Stokes (RANS) modeling of the flow of non-Newtonian slurry in a pipe was conducted using the Star-CCM+ software. The k-ε model was used for the flow turbulence and the viscosity of the working fluid was modeled using the Herschel-Bulkley rheology equation. Various flow conditions were modeled ranging from laminar to turbulent flow, with Reynolds numbers of 550, 3400, and 25,300, respectively. It was observed that RANS simulations could not generate results in good agreement with the experimental data under the specified conditions. Simulations predicted inaccurate shear in near-wall regions in the laminar case and inaccurate shear in the flow core regions in all regimes of the flow. Therefore, we propose a modified definition of viscosity for the non-Newtonian fluids which is based on a non-linearity coefficient obtained from the rheogram of the fluid during the simulation. Significant improvements were obtained through application of this model in simulation of flow in a periodic domain for laminar, transitional, and turbulent regimes of the flow.

INTRODUCTION

Presently millions of gallons of radioactive waste are stored in underground tanks at various U.S Department of Energy (DOE) sites (Gokaltun et al., 2012) and DOE is in the process of transferring the waste from single shell tanks to double shell tanks (Meyer et al., 2005 and Gokaltun et al., 2012). Meyer et al. (2005) introduced two types of simulants for the PJM systems in the Hanford site 1) a Laponite-based simulant with the Laponite concentration typically about 2 wt% and the density slightly greater than that of water, 2) a Kaolin-bentonite simulant with 80% kaolin and 20% bentonite powder mixed to various solids concentrations in water. Simulant development efforts are summarized in their work and in Poloski et al. (2004). Peltier et al. (2015) considered the 1.5 wt% Laponite-based simulant for

the slurry in PJM systems, which according to Escudier et al. (1996), obeys the Herschel–Bulkley rheological model.

Literature contains a number of valuable experimental investigations on non-Newtonian fluids such as given in Bingham (1922), Dodge and Metzner (1959), Thomas, (1963a, b), Pinho and Withelaw (1990), Escudier et al. (1996), Poloski et al. (2004), and Meyer et al. (2005). Some of these investigations such as the one by Bingham (1922), Herschel and Bulkley (1926), and Cross (1965) led to development of popular viscosity models for non-Newtonian fluids that are extensively used in computational investigations today. However, according to Gavrilov and Rudyak (2014), amount of available experimental data on non-Newtonian flows is insignificant compared to exploding efforts towards numerical simulations.

There have been efforts published in the literature to improve the accuracy of numerical algorithms in the prediction of flow variables and parameters of Non-Newtonian fluids. Wilson and Thomas (1986) improved the theory of the power-law and Bingham plastic categories for the log-law region of the velocity profile towards better prediction of the wall friction coefficient. Their analysis was based on drag reduction associated with non-Newtonian fluids and colloidal suspensions, as was first reported by Toms (1948), according to Andrade et al. (2007). This modification reflected enhanced viscosity effects at the small time and length scales of the dissipative micro-eddies. Soto and Shah (1976) developed an algorithm for the simulation of an entrance flow of a yield-power-law fluid. Their algorithm showed to provide results in good agreement with analytical solutions for different yield stress and power-law exponents. Bartosik (2010) applied the theory of Wilson and Thomas (1985), which described the change of the boundary layer thickness and suppression of turbulence in the boundary layer for the slurry flow with very fine solid particles. Bartosik (2010) employed a k-ε turbulence model with modified damping functions and compared the performance of power-law and Herschel and Bulkley models in the simulation of Kaolin slurry. He found that Herschel and Bulkley better describes the shear stress at the low shear deformation rate. Gavrilov and Rudyak (2014) improved the prediction of a specific k-ε turbulence model by adding an extra term to the definition of the shear rate and obtained results in close agreement with data obtained from a direct numerical simulation (DNS) study; however, applicability of this model to the laminar flow is under question due to its dependence on the dissipation rate of the turbulent kinetic energy.

Despite these significant contributions, there is still a need to find a universal model to define the viscosity properly in the entire computational domain for both laminar and turbulence flows in a wide range of the Reynolds number and regardless of the flow conditions and geometry. The present work given in this paper relies on the fundamental theory of the Non-Newtonian fluids which relates the stress to the strain rate in order to develop an algorithm that can improve the predictions of the k-ε turbulence model. The core of this algorithm is the Herschel and Bulkley (H-B) model of viscosity and we aim to obtain modification that spans the entire computational domain and works for a wide range of Reynolds numbers. This

fundamental approach is solely based on the property of the fluid and unlike the methods mentioned earlier it does not change the structure of the turbulence model or the deformation of the flow. For this reason, the proposed algorithm has the capability to improve the numerical predictions for both laminar and turbulent flows.

THEORY AND HYPOTHESIS

According to Escudier et al. (2005) and Meyer et al. (2005) the slurry fluid in Hanford site can be categorized as a viscoplastic material. Figure 1(a) shows the non-linear variation of the stress against the strain rate after the yield stress is achieved in the flow. The mathematical expression for this stress-strain relationship is given as

$$|\tau| = \tau_Y + k\,\Upsilon^n \,. \qquad \text{Eq.(1)}$$

In this expression, τ, τ_y, k, γ, and n are the shear stress, the yield shear stress, the consistency, the shear rate, and the power exponent, respectively. In addition, $|\tau|$ shows the magnitude of the shear stress. It is possible to define a coefficient, α, as the ratio of the area under the stress-strain curve of a Bingham plastic fluid to the area under the Newtonian curve, as shown in Figure 1(a) and expressed by Eq.(2). In other words, α is the ratio of the dissipation rate of the kinetic energy for non-Newtonian fluid over the pseudo-Newtonian fluid. We used the term "non-linearity coefficient" for α as it shows the deviation of the kinetic energy dissipation of non-Newtonian fluid from that of a Newtonian fluid. The term "pseudo-Newtonian" is used since this scholar represents an imaginary Newtonian fluid which is constructed from the rheogram of a non-Newtonian fluid. The theory of Wilson and Thomas (1985) states that as far as dissipative eddies of a turbulent flow are concerned, the non-Newtonian fluid acts as if it were a Newtonian fluid with viscosity of $\alpha \times \eta$ (which will give the same area under the curve, and hence the same dissipation rate as that for the non-Newtonian). This method is similarly applied to laminar flows in the absence of eddies, since dissipation of energy occurs by the action of viscosity regardless of the flow regime.

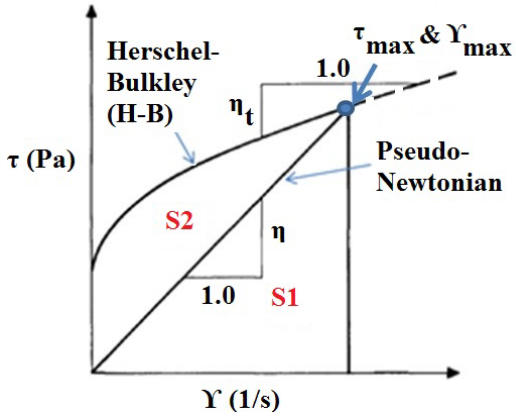

(a)

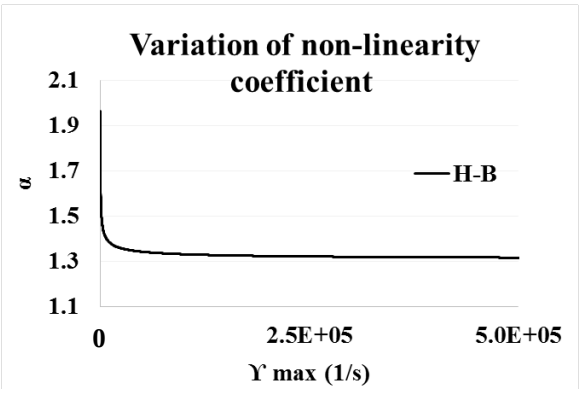

(b)

Figure 1. Characteristics of the non-Newtonian fluids. (a) the typical rheogram (b) eddy size in turbulent flow (Wilson and Thomas, 1986).

Eq.(3) shows the mathematical expression for the division of area defined for every step of the solution. In this expression the subscript "max" refers to the highest point on the rheogram profile. It must be noted that in every iteration, a new rheogram will be obtained from the solution of flow equations and the solution will dynamically adapt to the new rheogram. By replacing the stress term from Eq.(1) the expression to the right of the second equality sign in Eq.(3) was obtained. More derivations lead to a simple relation for α, as shown in Eq.(4), that depends on one variable. i.e., the maximum shear rate (Υ_{max}), and the rest are constant parameters. This dependency is shown for a wide range of the variation of Υ_{max} in Figure 1(b), where α varies between 1.3 to 2. Later, by utilizing the well know shear-strain relationship, i.e., $|\tau| = \mu \times \Upsilon$, we defined a pseudo-Newtonian viscosity as the slope of the hypotenuse of S1 triangle shown in rheogram of Figure 1. This quantity is expressed by Eq.(5).

$$\alpha = \frac{S1+S2}{S1} \qquad \text{Eq.(2)}$$

$$\alpha = \frac{\int_0^{\Upsilon max}(\tau.d\Upsilon)_{H\text{-}B}}{0.5\times(\Upsilon_{max})_{H\text{-}B}\times(\tau_{max})_{H\text{-}B}} = \frac{\int_0^{\Upsilon max}[(\tau_y+K\,\Upsilon^n)d\Upsilon]_{H\text{-}B}}{0.5\times(\Upsilon_{max})_{H\text{-}B}\times[(\tau_y+K\,\Upsilon^n)\Upsilon_{max}]_{H\text{-}B}} \qquad \text{Eq.(3)}$$

$$\alpha = 2\times\frac{\tau_y+\frac{K\,(\Upsilon_{max})^n}{n+1}}{\tau_y+K\,(\Upsilon_{max})^n} \qquad \text{Eq.(4)}$$

$$\mu_{psudo\_Newt.} = \frac{\tau_{H\text{-}B\text{-}max}}{\Upsilon_{max}} = \frac{\tau_Y}{\Upsilon_{max}} + k\,\Upsilon_{max}^{(n-1)} \qquad \text{Eq.(5)}$$

According to Wilson and Thomas (1985), dissipation can occur in the entire computational domain and predominantly in the viscous sub-layer, where only dissipative eddies can be present. Therefore, by multiplying the α coefficient with the pseudo-Newtonian viscosity, it is possible to modify the viscosity, μ, in the entire domain in an iterative and corrective fashion. This modification is not needed for the large eddies since large eddies do not participate in viscous dissipation. Therefore, a model with the following formulation is proposed:

$$\mu = \begin{cases} \mu_{H-B} = \frac{|\tau|}{\Upsilon} = \frac{\tau_Y}{\Upsilon} + k\,\Upsilon^{(n-1)} & \varepsilon_{H-B} \le \varepsilon - \mathrm{THS} \\ \alpha \times \mu_{psudo\_Newt.} & \varepsilon_{H-B} > \varepsilon - \mathrm{THS} \end{cases} \qquad \text{Eq.(6)}$$

In this formulation the H-B viscosity, as is defined on the first line of the Eq.(6), is obtained by using the shear-strain relations ship, i.e., $|\tau| = \mu \times \Upsilon$, imposed on the Eq.(1). This viscosity function is provided to the code as part of the input property of the fluid. The parameter ε-THS is defined as the threshold for the dissipation rate. We set this threshold to zero to engage the entire dissipation range (all dissipative scales) in the modification of viscosity. However, sensitivity of the model can be further reduced by increasing the ε-THS values. In the laminar flow simulation, the entire domain will be affected.

The following algorithm is executed to implement the α method in the STAR-CCM+ CFD application:

1. Initialize the solution with a constant viscosity
2. Update the entire flow field by solving the governing equations
3. Switch to the Herschel-Bulkley method
4. Update the entire flow field by solving the governing equations
5. Update the rheogram and correct the viscosity
6. Go to step 4 and continue until converged solution is obtained.

GOVERNING EQUATIONS

In this section, the governing equations of the turbulence model and the method of Gavrilov and Rudyak (2014) are briefly explained. Eqs. (7 - 11) show the expressions for the conservation of continuity and momentum and the standard k-ε model. In these equations all vectors and scalars represent mean field variables except for the primed variables, which represent fluctuations. The values of model constants, σ_k and σ_ε, in STAR-CCM+ are 1.0 and 1.3, respectively. In addition, μ_t is the turbulent viscosity defined by $\mu_t = \rho\, C\mu\, k\, T$, where, the values of Cμ is 0.09, and T is the turbulent time scale defined by Eq.(13).

$$\frac{\partial(\rho)}{\partial t} + \nabla.(\rho u) = 0\ , \qquad \text{Eq.(7)}$$

$$\frac{\partial(\rho u)}{\partial t} + \rho u.\nabla u = -\nabla P + \nabla.(2\,\mu\, S) + \nabla.(-\rho\langle \acute{u}\acute{u}\rangle) + \nabla.(2\,\acute{\mu}\,\acute{S})\ , \qquad \text{Eq.(8)}$$

$$S = \frac{1}{2}\left[\nabla u + (\nabla u)^T\right] \text{ and } \acute{S} = \frac{1}{2}\left[\nabla \acute{u} + (\nabla \acute{u})^T\right] \qquad \text{Eq.(9)}$$

$$\frac{\partial(\rho k)}{\partial t} + \frac{\partial}{\partial x_j}(\rho k\, u_i) = \frac{\partial}{\partial x_j}\left[(\mu + \frac{\mu_t}{\sigma_k})\frac{\partial(k)}{\partial x_j}\right] + G_t - \rho\varepsilon \qquad \text{Eq.(10)}$$

$$\frac{\partial(\rho\varepsilon)}{\partial t} + \frac{\partial}{\partial x_j}(\rho\varepsilon\, u_i) = \frac{\partial}{\partial x_j}\left[(\mu + \frac{\mu_t}{\sigma_\varepsilon})\frac{\partial(\varepsilon)}{\partial x_j}\right] + C_1\frac{\varepsilon}{k}[G_t] - C_2{}^{*}\rho\frac{\varepsilon^2}{k} \qquad \text{Eq.(11)}$$

$$G_t = (-\rho\overline{\acute{u}_i\acute{u}_j})\frac{\partial u_j}{\partial x_j} = \mu_{t.}|S|^2 - \frac{2}{3}\rho k\,\nabla.u - \frac{2}{3}\mu_{t.}(\nabla.u)^2 \qquad \text{Eq.(12)}$$

$$T = \max\left(\frac{k}{\varepsilon}, C_t\sqrt{\frac{\upsilon}{\varepsilon}}\right),\ C_t = 1 \qquad \text{Eq.(13)}$$

In the RANS framework, the mean values of field variables are solved and information about fluctuation components are lost. One such quantity is the shear rate, which has special importance for the calculation of viscosity in the H-B model. In the shear-rate correction method of Gavrilov and Rudyak (2014), the fluctuation component of the shear rate tensor is recovered by an approximation. This approximation, i.e., $\rho\varepsilon = \mu\langle 2\,\acute{S}ij\,\acute{S}ij\rangle$, is in accord with the definition of the isotropic dissipation rate introduced by Tennekes and Lumley (1983) and relates the mean dissipation rate of turbulence (ε) to the fluctuation component of the shear rate. Consequently, modified expressions for the shear rate and its extension to the H-B model are obtained, as shown by Eq.(14) and Eq.(15), respectively.

$$\gamma^2_{mod.} = 2\,S_{ij}S_{ij} + \langle 2\,\acute{S}_{ij}\acute{S}_{ij}\rangle = 2\,S_{ij}S_{ij} + \frac{\varepsilon}{\nu} \qquad \text{Eq.(14)}$$

$$\mu_{H-B\,mod.} = \frac{|\tau|}{\gamma_{mod.}} = \frac{\tau_Y}{\gamma_{mod.}} + k\,\gamma_{mod.}^{(n-1)} \qquad \text{Eq.(15)}$$

In this expression γ and ν are the shear rate and the kinematic viscosity, respectively. In the present work, application of the α method (direct viscosity correction) and the shear rate correction is investigated in the numerical simulation of a pipe flow that is explained hereafter.

SIMULATION METHODOLOGY

Flow of 1.5 wt% Laponite-based simulant inside a pipe was considered. Experimental and computational investigations of this flow in different regimes, i.e., laminar, transitional, and turbulent, were performed by Escudier et al. (1996) and Peltier et al. (2015), respectively. Figure 2 shows the periodic axisymmetric computational domain along with the line probe used for measurements and the computational grid generated for our simulations. Boundary conditions, as well as dimensions of the domain and properties of the fluid, are illustrated in Table 1.

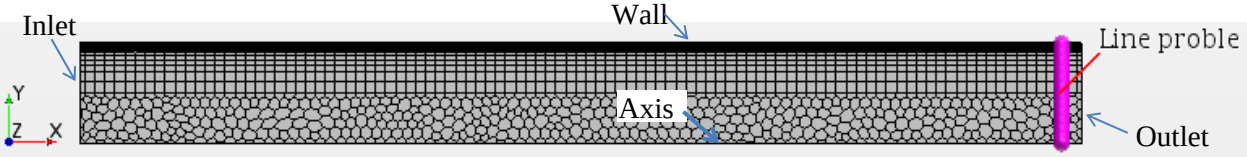

Figure 2. Two-dimensional computational domain containing 2177 cells.

Table 1. Boundary conditions, geometry, and fluid properties in the RANS simulations

CASE	RE = 550	RE = 3400	RE = 25300
Boundary conditions	Periodic	Periodic	Periodic
Inlet velocity, v_i (m/s)	0.52	1.09	2.03
Mass flow rate at interface, $\dot{m}$ (kg/s)	4.08	8.56	15.94
Pressure at outlet	1atm	1atm	1atm
Fluid properties			
Density, ρ(kg/m^3)	1000		
Yield stress, τ_y (pa)	4.42		
Consistency factor, k (Pa.s^n)	0.242		
Exponent, n	0.534		
Pipe dimensions			
Length (m)	0.5		
Diameter (m)	0.1		
Number of prism layer	20		
Non-slip wall for all cases			

According to the proposed algorithm above, the simulation was initialized with a constant viscosity of 8.8×10^{-4} Pa.s (for water in standard condition) and in the second iteration the field function for the proposed viscosity model, i.e., Eq.(6), and shear rate correction, i.e., Eq.(15), was introduced to the STAR-CCM+. Hereafter, the authors will use the acronym of "SRC" method for the shear rate correction method of Gavrilov and Rudyak (2014) for the purpose of brevity. Axial viscosity was obtained at the location x=0.98l. Axial velocities on the line probe in this location along with volume average of viscosity were our criteria for the system to reach steady state condition. Data associated with field variables, such as axial velocity, wall-averaged viscosity, and shear rate at wall were reported once the mean values of criteria did not change with more iterations.

SIMULATION RESULTS

Simulation results with different Reynold numbers are shown in Figure 3**.** In the case of the laminar flow (Re = 550), prediction obtained by the alpha method is significantly better than the original H-B method in 0.03<r<0.05m. Increase of viscosity and reduction of shear rate in this region is a consequence of implementation of the alpha method. However, results are not in good agreement in the core flow region, i.e., in 0<r<0.03m. Over-predicted shear rate is the underlying factor for continuous increase of velocity towards the axis of the pipe. For the H-B method, shear rate is over predicted near the wall and under predicted in the core flow region.

For the transitional flow (Re = 3400), results show significant improvement of the axial velocity profile obtained from the alpha method. Improvements are observed almost over the entire length of the probe and are more pronounced in the core flow region, i.e., in 0<r<0.0275m. In this region, the H-B and shear correction (SRC) methods, predicted a flat profile, as an indication of zero shear stress. These models, over predicted the velocity on the lower half length of the probe, i.e., in 0.0275<r<0.05m.

For the turbulent flow (Re = 25300), all models predicted the velocity profile precisely in the near wall region, i.e., in 0.045<r<0.05m. In median regions, i.e., in 0.0225<r<0.0475m, numerical predictions are close to each other, although the α method resulted in better prediction by generating lower velocities. In the core flow regions, i.e., in 0<r<0.0225m, all methods over predicted the velocities. Flat velocity profiles were obtained from the H-B and SRC methods, unlike the α method, which predicted a continuous trend of increase of axial velocity. This analysis confirms that the shear rate predicted by the α method is in better agreement with the shear rate of the experiment.

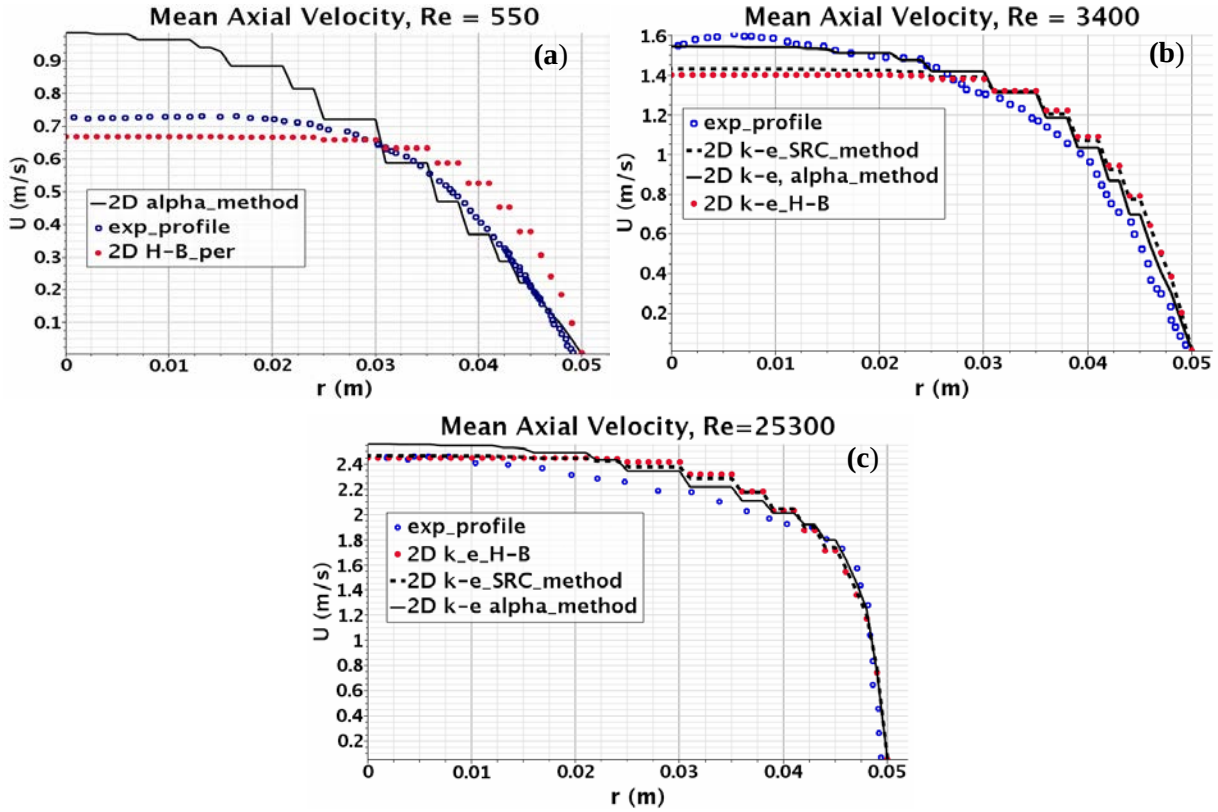

Figure 3. Profile of axial velocity at X=0.98 L in laminar (Re = 550), transitional (Re = 3400), and turbulent regimes (Re = 25300).

We extended our investigation to the analysis of the viscosity along the line probe. The purpose of this investigation was to better understand the differences observed earlier regarding the profiles of velocities predicted by different models. Figure 4 shows the variation of viscosity along the probe line for the three flow regimes under investigation in this study. For each regime, the viscosity obtained from the α method, also called as α-viscosity, is shown in red dots and is a constant value. This scalar was multiple orders of magnitude smaller than the viscosity values predicted in the flow core regions by H-B and SCR methods. In addition, Figure 4(a-c) show a descending trend of the α-viscosity with increasing Reynolds number. This trend is in accord with significantly higher shear rate at the wall region for a turbulent flow in comparison to a laminar flow.

In the laminar flow shown in Figure 4(a), we observed an increase of the H-B viscosity to the α-viscosity near the wall region, (0 <Y< 0.01m), where Y represents the distance from the wall. This increase of the viscosity is in accord with lower axial velocities obtained by the α method for Re = 550 in this region, as shown in Figure 3(a). However, continuous drop of the viscosity after Y= 0.01m resulted in continuous increase of the shear rate and significantly higher axial velocities towards the centerline.

For the transitional flow, i.e., Re = 3400, Figure 4(b) shows slight increase of the viscosity in 0<Y<0.01m by the α method which resulted in better predictions in this

region, similar to the laminar flow. Further away from the wall, lower viscosities by the α method resulted in higher velocities, which better agreed with the experimental data. One notable fact is that similar to the α method, the SCR method reduced the viscosity; however, inadequate reduction of the viscosity resulted in small improvements in only the flow core region (0<Y<0.25m).

In the case of the turbulent flow, i.e., Re = 25,300, similar values of viscosity were obtained from all the models in the vicinity of the wall (0<Y<0.01m). This explains why numerical profiles in Figure 3(c) presented almost the same values of axial velocity; however, profiles of axial velocity obtained by the H-B and SRC follow each other closely towards the symmetry axis of the pipe, even though the viscosity profiles depart rapidly and significantly from each other on the mid length of the probe, i.e., at Y= 0.25m. Weakened action of the viscosity in comparison to the inertia effects in turbulent flows can explain this suppressed effect in the regions away from the solid boundary.

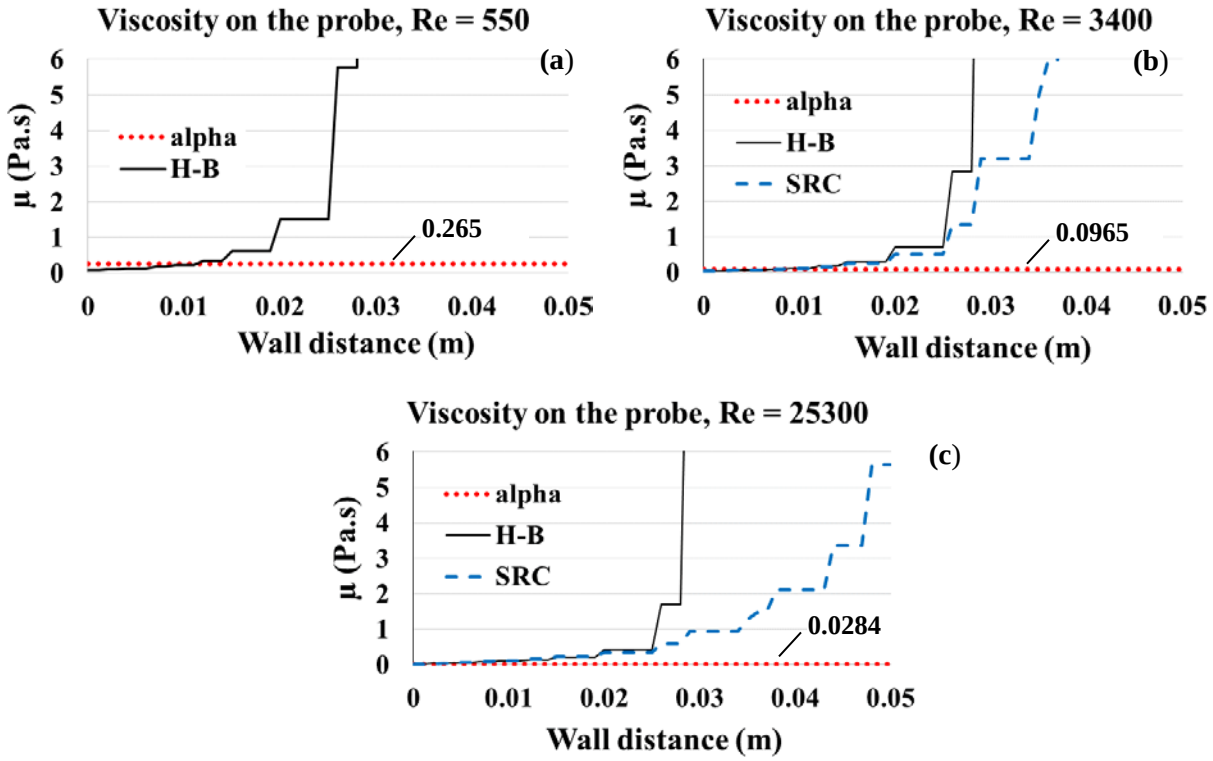

Figure 4. Variation of viscosity in radial direction at X=0.98 L in laminar (Re = 550), transitional (Re = 3400), and turbulent regimes (Re = 25300).

DISCUSSION AND SUMMARY

In previous sections, we presented a method to obtain and utilize a constant viscosity value during each of our RANS simulations. This method was used to reduce the H-B viscosity in a large portion of the domain in all simulation cases. In some cases, the method worked to increase the viscosity in small portions of the computational domain. In fact, we presented non-Newtonian fluid simulations using the H-B and SRC methods versus pseudo-Newtonian fluid simulations using the α method. Through the α method, varying viscosity of the fluid was replaced with a constant viscosity that could significantly improve the accuracy of the simulation results. In addition, the α method alleviated the singularity problem of the H-B method. The H-B method in its original form, i.e., in $\mu = \tau_y / \dot{\gamma} + k\dot{\gamma}^{(n-1)}$, is subject to singularity in the core flow regions, where shear rate approaches zero. This singularity is not clear from Figure 4(a-c) since the y-axis on all of the plots are limited to 6 Pa.s for better comparisons.

Our analysis was founded on the H-B model as the background model and modifications were implemented based on the results of this model. An algorithm was developed for implementation of the proposed model, which found the α and the pseudo-Newtonian viscosity from the updated rheogram of the H-B model in each iteration. For this reason, under the circumstances that the H-B model over predicts or under predicts the rheogram, utilization of over-predicted or under-predicted values of α or pseudo-Newtonian viscosity may occur in each iteration.

Results reported in this paper, indicated improved velocity profiles for the laminar, transitional, and turbulent regimes of the flow. In the laminar flow (Re = 550), results of the H-B model were improved in the range of $0.5 < r/R < 1$. In the lower range, excessive drop of the viscosity resulted in continuous increase of shear rate and the axial velocity. For the transitional (Re = 3400) the velocity profile was improved over the entire range, i.e., $0 < r/R < 1$ and in the turbulent flow (Re = 25300), improvements were in the range of $0.45 < r/R < 1$. However, the shear rate was better predicted in the core region, even though higher velocities were predicted by the α method. Finally, the use of the α method for the laminar flow must be accompanied with caution. It is suggested to use the α method in high shear rate regions close to the solid boundary.

REFERENCES

Andrade L.C.F., Petronílio J.A., de A. Maneschy C.E., de A. Cruz D.O., 2007, The Carreau-Yasuda Fluids: a Skin Friction Equation for Turbulent Flow in Pipes and Kolmogorov Dissipative Scales, Journal of the Brazilian Society of Mechanical Science and Engineering, Vol. 29, Issue 2, p163

Bingham E.C., Fluidity and Plasticity, McGRAW-Hill Inc., 1922

Bartosik A., 2010, Application of Rheological Models in Prediction of Turbulent Slurry Flow, Flow Turbulence, and Combustion, Volume 84, pp 277–293

Cross, M.M., 1965, Rheology of non-Newtonian fluids: A New Flow Equation for Pseudoplastic Systems, Journal of Colloid Science, pp 417-437

Dodge D.w., Metzner A.B., 1959, Turbulent Flow of Non-Newtonian Systems, AIChE journal, Volume 5, Issue 2, p189

Escudier M.P., Presti F., 1996, Pipe Flow of a Thixotropic Liquid, J. Non-Newtonian Fluid Mech., volume 62, PP. 291-306

Escudier M.P., Poole R.J., Presti F., Dales C., Nouar C., Desaubry C., Graham L., Pullum L., 2005, Observations of Asymmetrical Flow Behaviour in Transitional Pipe Flow of Yield-Stress and Other Shear-Thinning Liquids, Journal of Non-Newtonian Fluid Mechanics, Volume 127, pp 143–155

Gokaltun S., McDaniel D. and Roelant D., 2012, Three Dimensional Simulations of Multiphase Flows Using a Lattice Boltzmann Method Suitable for High Density Ratios – 12126, WM2012 Conference, February 26- March 1 2012, Phoenix, AZ

Gavrilov A.A., Rudyak V.Y., 2014, A Model of Averaged Molecular Viscosity for Turbulent Flow of Non-Newtonian Fluids, Journal of Siberian Federal University, Journal of Mathematics & Physics, Voulem 7, Issue 1, pp 46–57

Herschel W.H., Bulkley R., 1926, Kolloid-Zeitschrift, Volume 39, Issue 4, pp 291–300, doi:10.1007/BF01432034

Meyer P.A., Kurath D.E., Stewart C.W., 2005, Overview of the Pulse Jet Mixer Non-Newtonian Scaled Test Program, PNWD-3677, WTP-RPT-127 Rev. 0

Poloski A., Smith H., Smith G., Calloway T., 2004, Technical Basis for HLW Vitrification Stream Physical and Rheological Property Bounding Conditions. WTP-RPT-100 Rev. 0, Battelle – Pacific Northwest Division, Richland, Washington.

Peltier J, Andri R, Rosendall, Inkson N., Lo S., 2015, Evaluation of RANS Modeling of Non-Newtonian Bingham Fluids in the Turbulence Regime Using STAR-CCM+®,

Advanced Simulation & Analysis, BecthelNuclear, Security & Environmental, Cd-adapcoTM , Conference: STAR Global Conference 2015.

Pinho F.T., Whitelaw J.H., 1990, Flow of Non- Newtonian Fluid in A Pipe, Journal of Non-Newtonian Fluid Mechanics, Volume 34, pp 129-144

Rudman M., Blackburn H.M., Graham L.J.W., Pullum L., 2004, Turbulent Pipe Flow of Shear-Thinning Fluids, J. Non-Newtonian Fluid Mechanics, Volume 118, pp 33–48

Soto R.J., Shah V.L., 1976, Entrance Flow of a Yield-Power Law Fluid, Journal of Applied Science Research, Volume 32

Tennekes H., Lumley J.L., “A First Course in Turbulence”, The MIT Press, 1972, pp 64-66

Toms B.A.,1948, Some Observations on the Flow of Linear Polymer Solution through Straight Tubes at Large Reynolds Number, Proceedings of 1st Conference on Rheology, Vol.2, North Holland, Amsterdam, p135.

Thomas, D.G., 1963a, Non-Newtonian Suspensions: Part 1, Physical Properties and Laminar Transport Characteristics, Industrial and Engineering Chemistry, pp 55-18.

Thomas, D.G., 1963b, Non-Newtonian Suspensions: Part 11, Turbulent Transport Characteristics, Industrial and Engineering Chemistry, pp 55-27

Wilson, K.C., Thomas A.D., 1985, A New Analysis of the Turbulent Flow of Non-Newtonian Fluids, The Canadian Journal of Chemical Engineering, Volume 63